CELL CYCLE
2016, VOL. 15, NO. 18, 2454–2463
http://dx.doi.org/10.1080/15384101.2016.1201255

Taylor & Francis
Taylor & Francis Group

REPORT

Elevated intracellular pH appears in aged oocytes and causes oocyte aneuploidy associated with the loss of cohesion in mice

Jin-Mei Cheng[a,b], Jian Li[a,b], Ji-Xin Tang[a,b], Su-Ren Chen[a], Shou-Long Deng[a], Cheng Jin[a,b], Yan Zhang[a], Xiu-Xia Wang[a], Chen-Xi Zhou[a], and Yi-Xun Liu[a]

[a]State Key Laboratory of Stem Cell and Reproductive Biology, Institute of Zoology, Chinese Academy of Sciences, Beijing, China; [b]University of Chinese Academy of Sciences, Beijing, China

ABSTRACT

Increases in the aneuploidy rate caused by the deterioration of cohesion with increasing maternal age have been well documented. However, the molecular mechanism for the loss of cohesion in aged oocytes remains unknown. In this study, we found that intracellular pH (pH_i) was elevated in aged oocytes, which might disturb the structure of the cohesin ring to induce aneuploidy. We observed for the first time that full-grown germinal vesicle (GV) oocytes displayed an increase in pH_i with advancing age in CD1 mice. Furthermore, during the *in vitro* oocyte maturation process, the pH_i was maintained at a high level, up to ~7.6, in 12-month-old mice. Normal pH_i is necessary to maintain protein localization and function. Thus, we put forward a hypothesis that the elevated oocyte pH_i might be related to the loss of cohesion and the increased aneuploidy in aged mice. Through the *in vitro* alkalinization treatment of young oocytes, we observed that the increased pH_i caused an increase in the aneuploidy rate and the sister inter-kinetochore (iKT) distance associated with the strength of cohesion and caused a decline in the cohesin subunit SMC3 protein level. Young oocytes with elevated pH_i exhibited substantially the increase in chromosome misalignment.

ARTICLE HISTORY
Received 8 April 2016
Revised 7 June 2016
Accepted 8 June 2016

KEYWORDS
aging; alkalinization; chromosome aneuploidy; cohesion; oocytes; pH_i

Introduction

Aneuploidy is a leading cause of pregnancy loss and an aggravating source of developmental disabilities and mental retardation in female mammals.[1-3] Most errors in chromosome number originate from eggs, and maternal age is well established as the key risk factor.[3-6] The incidence of aneuploid eggs dramatically increases with maternal age.[3,6]

Maternal age-related aneuploidy is a consequence of chromosome segregation errors during meiotic division.[7-9] In meiosis I, the crucial ploidy reduction step requires that sister kinetochores attach to microtubules emanating from the same spindle pole and that cohesin wrapped around chromosome arms dissolves. In meiosis II, chromosome segregation requires that sister kinetochores attach to opposite spindle poles and that centromeric cohesion dissolves.[10-12] The meiotic cohesin entrapped in sister chromatids through a ring-like structure is synthesized during the pre-meiotic S phase and must remain functional until meiotic resumption in adult life.[3,13] Cohesin deterioration has been characterized as a main cause of age-dependent aneuploidy.[3-5] However, the molecular mechanism for the loss of cohesion in aged oocytes is still elusive.

Old oocytes are characterized by a sequence of molecular and structural abnormalities, such as dysfunctions of intracellular Ca^{2+} regulation,[14-15] abnormal changes in mitochondrial structure,[16,17] and chromosome missegregation.[3,8] However, whether the intracellular pH (pH_i) of aged oocytes is abnormal remains unknown.

Mammalian cells maintain pH_i by means of several nearly ubiquitous mechanisms, including HCO_3^-/Cl^- exchangers of the anion exchanger (AE) gene family and Na^+/H^+ exchangers of the Na^+/H^+ exchanger (NHE) family. HCO_3^-/Cl^- exchangers export HCO_3^- in exchange for extracellular Cl^-, thereby correcting alkalosis; Na^+/H^+ exchangers extrude protons, thereby correcting acidosis.[18-20] The AE family HCO_3^-/Cl^- exchangers have been detected among polypeptide products of the Solute Carrier 4 (*SLC4*) gene superfamily, including *SLC4A1* (*AE1*), *SLC4A2* (*AE2*), *SLC4A3* (*AE3*) and *SLC4A9* (*AE4*).[21-23] *AE2* and *AE3* mRNAs are expressed in mouse preimplantation embryos starting at the 2-cell stage, while only *AE2* is present in eggs and 1-cell embryos.[24,25] Small growing oocytes isolated from juvenile mice do not exhibit pH_i-regulatory HCO_3^-/Cl^- exchanger activities and have a low pH_i; however, when the oocytes grow close to full size, the exchangers become active and have a high activity in mice.[26-28] However, after release from the first meiotic prophase arrest, the oocyte HCO_3^-/Cl^- exchanger activity begins to decrease slowly until it is almost undetectable in the metaphase I (MI)/metaphase II (MII) transition. In mice, the exchanger activity is reactivated only after egg activation.[29-31] Thus, fully grown germinal vesicle (GV)-stage mouse oocytes possess robust HCO_3^-/Cl^-

CONTACT Yi-Xun Liu, Ph.D. liuyx@ioz.ac.cn State Key Laboratory of Stem Cell and Reproductive Biology, Institute of Zoology, Chinese Academy of Sciences, Beijing 100101, People's Republic of China.

Color versions of one or more of the figures in the article can be found online at http://www.tandfonline.com/kccy

Supplemental data for this article can be accessed on the publisher's website.

exchanger activity that confers protection against alkalosis and is most likely mediated by AE2.[26,29,30]

To address the above questions, the pH_i values of oocytes from 1-, 3-, 6-, 9-, 12- and 15-month-old mice were measured using the pH-sensitive fluorophore BCECF-AM to analyze the effect of aging on the oocyte pH_i. We have demonstrated for the first time that the oocyte pH_i increases with mouse age. According to this result and the age-related aneuploidy, we put forward a hypothesis that the elevated pH_i in aged oocytes might be related to the increase in chromosome aneuploidy. To verify this hypothesis, the young oocyte pH_i was increased in the *in vitro* maturation process by adding 4,4′-diisothiocyanatostilbene-2,2′-disulfonate (DIDS), an inhibitor of HCO_3^-/Cl^- exchangers, to the culture medium after these oocytes in the GV stage were removed to Cl^--free media for a 10-minute (min) treatment.

Results

Increased aneuploidy in oocytes from aged mice

To investigate the effect of aging on aneuploidy in Swiss CD1 female mice, we counted the number of chromosomes in MII oocytes from 1- and 12-month-old mice (young and aged groups, respectively) using an in situ chromosome counting technique. We observed that the overall rate of aneuploidy in the young group was 4.9 % (4/82), whereas the rate in the aged group was 31.6 % (18/57), which was a significant increase ($P < 0.01$) (Fig. 1A). This result is consistent with the previous report in mice.[32] To investigate whether aneuploidy influenced germinal vesicle breakdown (GVBD) and polar body extrusion (PBE) of oocytes, we counted the number of GVBD and PBE at different times in the *in vitro* culture process using time-lapse live imaging. We observed that aged oocytes underwent GVBD and PBE with similar efficiencies and kinetics as young oocytes (Fig. 1B and C). Taken together, aging causes the increase in chromosome aneuploidy of MII oocytes.

Elevated oocyte pH_i in the aged mice

To address whether aging influences oocyte pH_i, we measured the pH_i of 519 full-grown and denuded GV oocytes from 1-, 3-, 6-, 9-, 12- and 15-month-old-mice using the pH-sensitive fluorophore BCECF-AM (Fig. 2A and B). We found that the pH_i was maintained at 7.2-7.3 in the 1-, 3-, 6-, and 9-month-old groups (n = 103, 112, 120, 73, respectively). In contrast, the pH_i increased 0.2-0.3 pH units in the 12- and 15-month-old groups (n = 64, 47, respectively) compared to the other groups (Fig. 2B). To determine whether the oocyte pH_i of the aged group was maintained at a high level in the subsequent phase, we then measured the pH_i values of GVBD, MI, and MII oocytes from the 1- and 12-month-old mice. As shown in Fig. 2C, regardless of the oocyte phase, compared to the 1-month-old group, the oocyte pH_i always increased 0.2-0.3 pH units and reached the level of ~7.6 in the 12-month-old group. Collectively, aging causes the increase in pH_i in mouse oocytes.

Decreased activity of the HCO_3^-/Cl^- exchanger in aged GV oocytes

Because the HCO_3^-/Cl^- exchanger runs in reverse on exposure to a Cl^--free solution, the oocyte pH_i increases in a Cl^-- free medium (Fig. 3A). To explore the reason for the increased pH_i in aged oocytes, we measured the activity of the HCO_3^-/Cl^- exchanger in GV oocytes from 1-, 3-, 6-, 9-, 12- and 15-month-old mice using the pH_i measurement on BCECF-loaded oocytes in a Cl^- removal assay. We found that GV oocytes exhibited a lesser pH increase upon Cl^- removal from the bathing media at 10 mins in the 12- and 15-month-old groups than in the 1-, 3-, 6- and 9-month-old groups (Fig. 3B). HCO_3^-/Cl^- exchanger activity is reported as the change in pH_i per min (pHU/min).[26,27] Through linear regression to compute the initial rate of intracellular alkalinization upon Cl^- removal, we found that the HCO_3^-/Cl^- exchanger activity of GV oocytes gradually decreased with increasing mouse age. The pHU/min was 0.058 in the 1-month-old group, but it decreased to 0.019

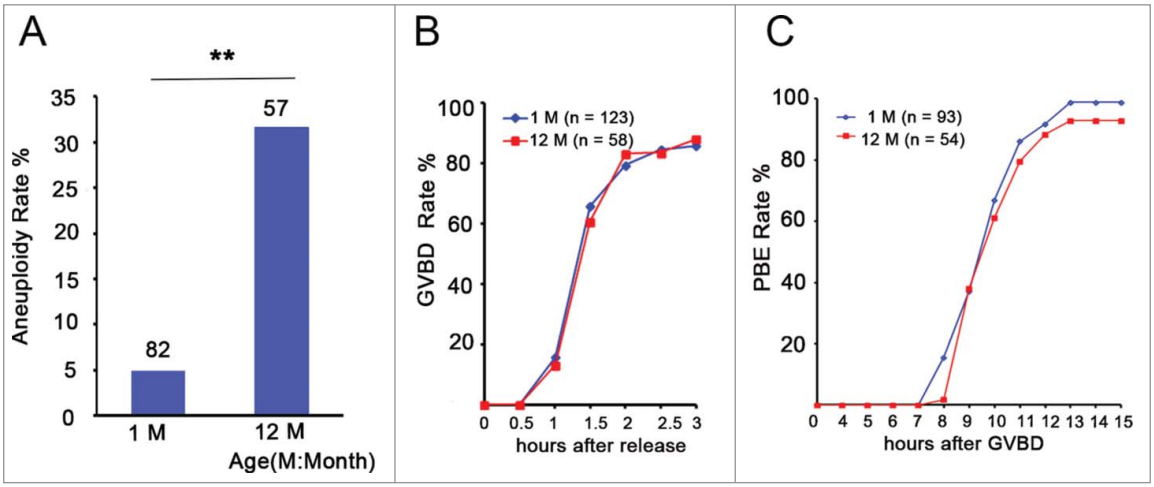

Figure 1. Aneuploidy is increased and has no effect on GVBD and PBE in aged oocytes. (A) Numbers analyzed are indicated above the bars. The data were analyzed using a chi-square test. The experiments were repeated more than 3 times. ** $P < 0.01$. (B) Kinetics of germinal vesicle breakdown (GVBD). GV-stage oocytes were isolated in M2 medium containing dbcAMP, which inhibits GVBD, and were released into inhibitor-free medium (at time = 0). The number of oocytes examined is indicated (n). (C) Kinetics of polar body extrusion (PBE). Oocytes that had undergone GVBD within 1.5 h after release into dbcAMP-free M16 medium were selected (at time = 0). The number of oocytes examined is indicated (n).

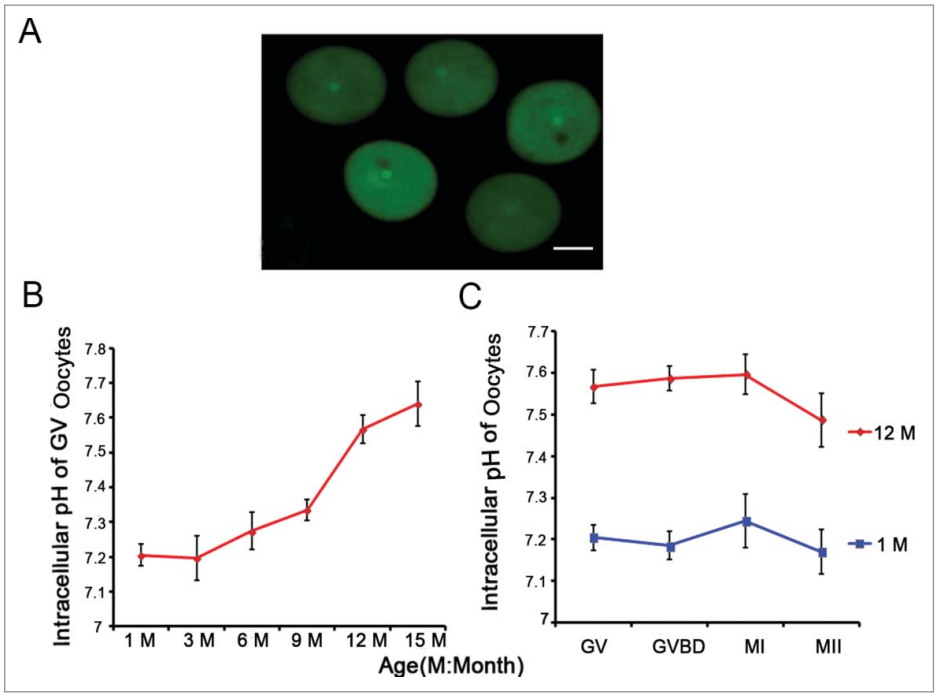

Figure 2. Aging leads to an increase in oocyte pH_i. (A) Full-grown and denuded GV oocytes were incubated with BCECF-AM to determine the pH_i. Scale bar, 30 μm. (B) Full-grown GV oocytes were released from the ovaries of mice of different ages and were then removed to low-lactate KSOM to stabilize for 15 min before their pH_i values were measured. (C) Oocytes from 1- and 12-month-old mice represent the young and aged groups, respectively. Full-grown GV oocytes were cultured in M16 medium for 2-2.5, 7.5-8 and 16-17 h to reach GVBD, MI and MII stages, respectively. In B and C, each point represents between 47 and 120 oocytes from 4 to 8 replicates. Data are presented as the means ± SEM.

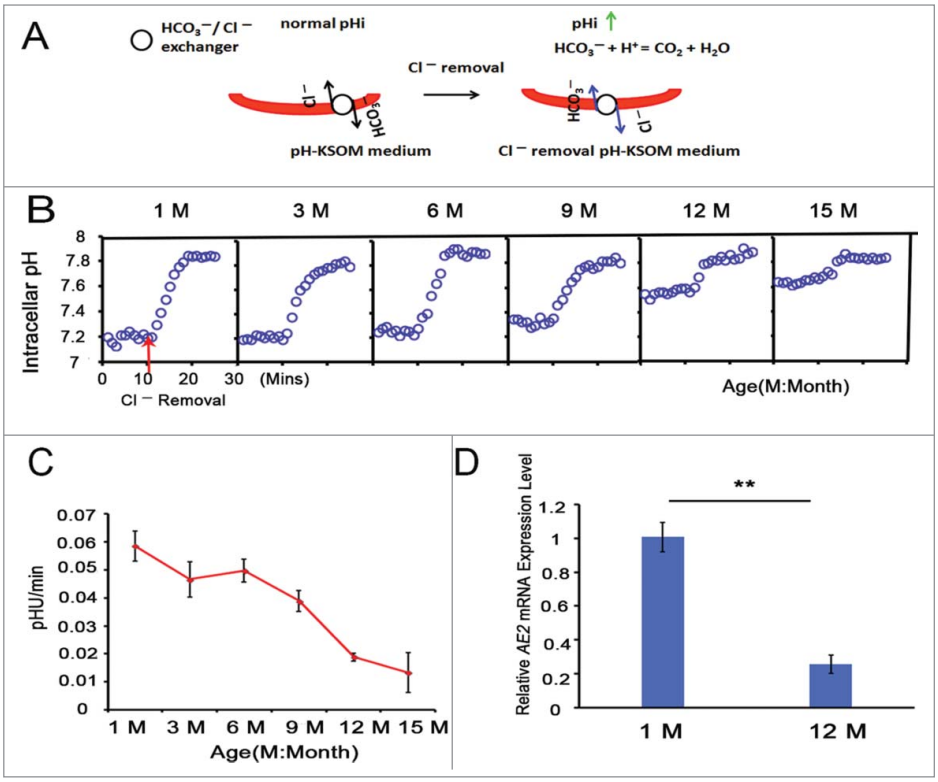

Figure 3. HCO_3^-/Cl^- exchanger activity is attenuated with advancing age in full-grown GV oocytes. (A) Model for the increase in oocyte pH_i using a Cl^- removal medium. (B) pH_i was monitored in denuded and full-grown GV oocytes from 1-, 3-, 6-, 9-, 12-, and 15-month-old mice; simultaneously, Cl^- was removed from the bathing medium at 10 mins, indicated by the *red arrow*; Mins: minutes, M: month. Traces shown are the means of all experiments performed. (C) The rate of pH_i increase upon C^- removal in GV oocytes was quantified, providing an indication of HCO_3^-/Cl^- exchanger activity. Each point represents between 47 and 120 oocytes from 4 to 8 replicates. (D) The relative *AE2* mRNA expression levels in GV oocytes from 1- and 12-month-old mice. *Gapdh* served as the internal control gene. The data are expressed as the means ± SEM. ** $P < 0.01$. Each experiment employed 80 oocytes and was repeated 4 times.

and 0.013 in the 12- and 15-month-old groups, respectively (Fig. 3C). In brief, aging leads to the reduction of HCO_3^-/Cl^- exchanger activity in full-grown GV oocytes.

In addition, real-time PCR analysis revealed that the relative *AE2* mRNA expression level was significantly decreased in the 12-month-old group compared to the 1-month-old group ($P < 0.01$), as shown in Fig. 3D.

Increases in sister inter-kinetochore (iKT) distance and chromosome aneuploidy in alkaline young oocytes

Considering the increased pH_i of old oocytes and the age-related aneuploidy, we speculated that elevated pH_i might be related to the high proportion of aneuploidy. Therefore, we elevated the pH_i of young oocytes during the *in vitro* maturation process by adding DIDS, a specific inhibitor of HCO_3^-/Cl^- exchangers (Supplemental Fig. S1A), to the culture medium after the GV stage oocytes were treated in Cl^--free media for 10 min (Fig. 4A). Meanwhile, GV oocytes were directly matured in the media without any addition and treatment, serving as the normal control group, and in the media supplemented with DIDS but without Cl^--free media treatment, serving as the DIDS control group. The sister iKT distance and the aneuploidy rate of their MII oocytes were measured using kinetochore and DNA immunofluorescent staining (Fig. 4B). The sister iKT distance increased significantly in the alkaline-treated group (0.39 μm, n = 795) compared to the normal and DIDS control groups (0.27 μm, n = 597, $P < 0.01$; 0.28 μm, n = 501, $P < 0.01$; respectively) (Fig. 4C). The aneuploidy rate was also higher in the alkaline-treated group (20.7 %, n = 82) than in the normal and DIDS control groups (4.9 %, n = 82, $P < 0.01$; 9.0 %, n = 67, $P < 0.05$; respectively) (Fig. 4D). Collectively, alkaline treatment of young oocytes causes the increases in chromosome aneuploidy and sister iKT distance.

Reduction of the chromosome-associated cohesin SMC3 in alkaline young oocytes

Structural maintenance of chromosomes 3 (SMC3) is a component of the cohesin complex.[5,13] To further explore the possible mechanism of increased iKT distance and aneuploidy rate in alkaline young oocytes, the expression of cohesin subunit SMC3 on chromosomes was detected in MI by immunofluorescence. The level of chromosome-associated SMC3 protein was obviously decreased in alkaline oocytes (Fig. 5A and B). Compared to the normal and DIDS control groups, the relative SMC3 fluorescence intensity on chromosomes was significantly decreased in the alkalinization group ($P < 0.01$) (Fig. 5B). In brief, alkalinization causes the reduction of SMC3 protein on chromosomes in young oocytes.

Chromosome misarrangement and normal attachment of kinetochores and microtubules in alkaline young oocytes

GV oocytes were microinjected with H_2B-RFP and MAP7-GFP cRNAs. Their chromosome track and spindle morphology were

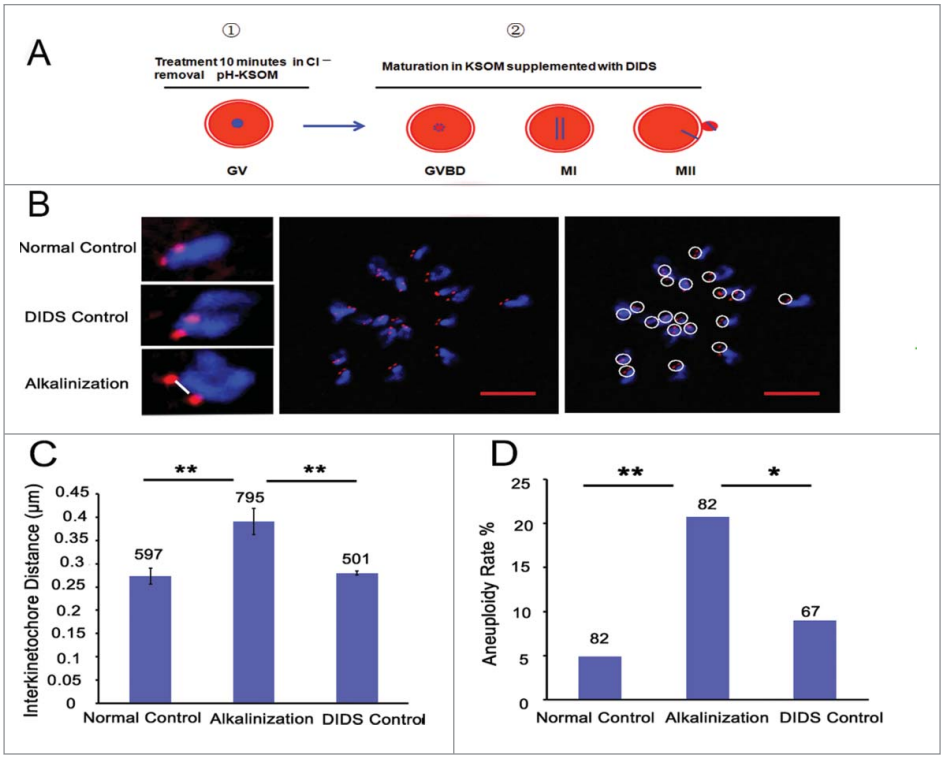

Figure 4. Alkaline treatment of young oocytes causes increases in chromosome aneuploidy and sister iKT distance. (A) Model for the process of alkaline treatment of young oocytes. 1) The pH_i of GV oocytes was increased. 2) The increased pH_i was maintained in different oocyte phases. (B) MII oocytes were spread in situ. A flattened z-stack series of images through a monastrol-treated egg (middle). Chromosomes were counted using a flattened z-stack series of images; the *white circle* represents a sister chromatid pair (right). Representative sister chromatid pairs from the normal control, DIDS control and alkaline treatment groups illustrating the increase in iKT distances; the *white line* shows the inner distance of the sister chromatid pair (left). Red, centromere (CREST); blue, chromatin (4,6-diamino-2-phenyl indole, DAPI). Bar = 5 μm. Alkalinization: oocytes were matured in a medium supplemented with DIDS after being removed to Cl^--free media for a 10-min treatment. Normal control: oocytes were matured in media without any addition and treatment. DIDS control: oocytes were matured in media supplemented with DIDS but without Cl^--free media treatment. In C and D, the numbers analyzed are indicated above the bars; $^{**}P < 0.01$; $^{*}P < 0.05$. In each experiment, the data shown represent more than 3 replications.

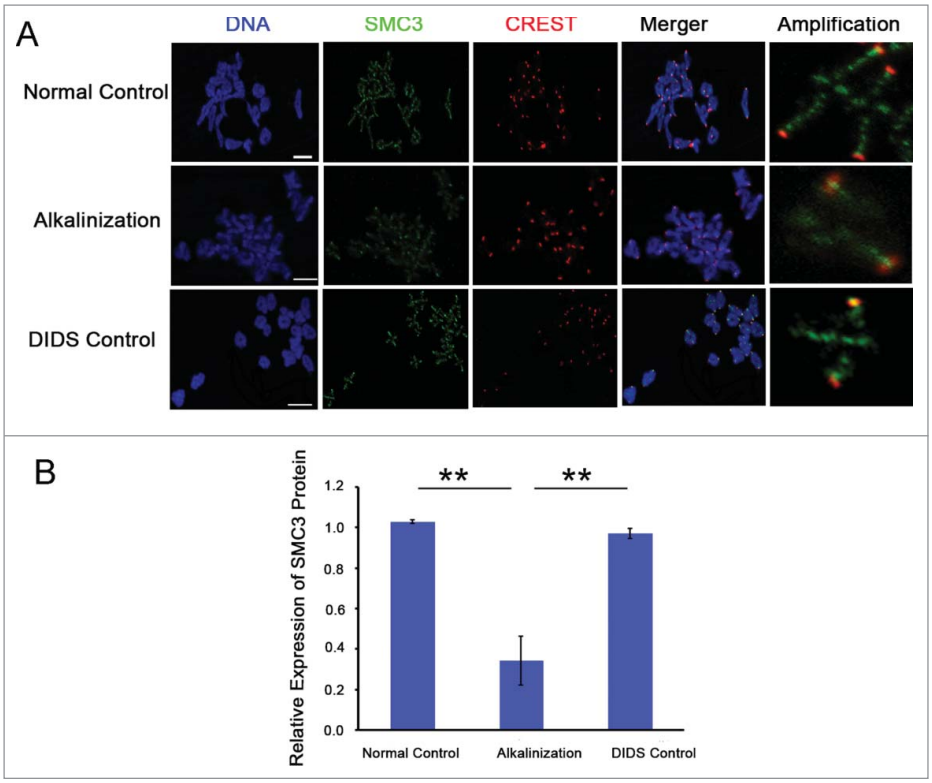

Figure 5. The expression level of SMC3 protein on chromosomes was obviously decreased in alkaline young oocytes. (A) The levels of chromosome-associated SMC3 protein were detected by immunofluorescence in normal, DIDS control and alkaline-treated oocytes at MI. Representative images show DNA (blue), CREST (red) and SMC3 (green). Scale bar, 5 μm. (B) SMC3 fluorescence intensity was quantified. Data are the means ± SEM, ** $P < 0.01$; ≥150 bivalents of each group were analyzed.

then observed during the *in vitro* maturation process via live cell imaging. The spindle morphology did not significantly change among the 3 groups (Fig. 6A). However, at the time of the onset of anaphase I, the number of oocytes with misaligned chromosomes significantly increased in the alkalinization group compared to the normal and DIDS control groups (74 %, 9 %, 13 %, respectively) (Fig. 6B). Meanwhile, in the alkalinization group, the time of anaphase I onset was delayed for most of the oocytes, occurring after 10 h of culture. Most of the oocytes from the normal and DIDS groups could enter anaphase I after 8-9 h of culture (Supplemental Fig. S2A and B).

Erroneous kinetochore–microtubule (KT-MT) interactions can also cause oocyte aneuploidy.[11,33] To exclude this reason, we assessed the KT-MT attachment status by immunostaining kinetochores and microtubules after destabilizing dynamic non-kinetochore microtubules with cold treatment in fixed MI oocytes (Fig. 6C). All confocal slices were examined, and each sister kinetochore pair was categorized as attached to microtubules emanating from a single pole (polar attached), attached to microtubule bundles at both poles (merotelic attached), or unattached to any cold-stable microtubule bundle (unattached) (Fig. 6D). We found that KT-MT interactions did not differ significantly across the 3 groups (Fig. 6D). One misaligned sister pair had a big sister iKT distance, and another pair had a single polar attachment between microtubule and kinetochore, as shown in Fig. 6C.

Discussion

In this study, we first report that the pH_i of full-grown GV oocytes increased with advancing age in CD1 mice and that the pH_i of oocytes was always maintained at a high level during the maturation process in 12- and 15-month-old mice (Fig. 2B and C). Two key issues are addressed in this discussion: (i) why increased pH_i is related to advancing age; and (ii) the possible mechanism for the elevated aneuploidy and deteriorated cohesion in old oocytes. HCO_3^-/Cl^- exchangers export HCO_3^- in exchange for Cl^- to correct any increase in the pH_i.[18,20,21] In mice, the HCO_3^-/Cl^- exchanger is fully active in full-grown GV oocytes.[26,27] In the present study, we measured the HCO_3^-/Cl^- exchanger activity of GV oocytes according to a previous Cl^- removal method[24,27,30] and found that the HCO_3^-/Cl^- exchanger activity decreased markedly in the GV oocytes of 12- and 15-month-old mice (Fig. 3C). Because of a lack of pH_i-regulatory exchange activities, the small growing oocytes isolated from juvenile mice and freed of their surrounding granulosa cells (denuded oocytes) have a low pH_i.[26,27] Inhibition of HCO_3^-/Cl^- exchange activity with DIDS disrupts intracellular pH homeostasis and markedly inhibits the development of embryos from 2 cells to blastocysts in mice.[25] Thus, we proposed that the decrease in HCO_3^-/Cl^- exchanger activity may be a cause for the elevated pH_i in aged oocytes. Furthermore, extreme changes in pH_i affect post-translational modification, particularly those changes that alter the protein charge in a site-specific manner, including phosphorylation and Lys acetylation.[34] Thus, it may be that the pH_i change conversely affects the post-translational modification of the HCO_3^-/Cl^- exchanger protein to increase the extent of pH change in aged oocytes.

The pH_i-regulatory HCO_3^-/Cl^- exchanger is active in full-grown GV oocytes and is most likely mediated by AE2 in

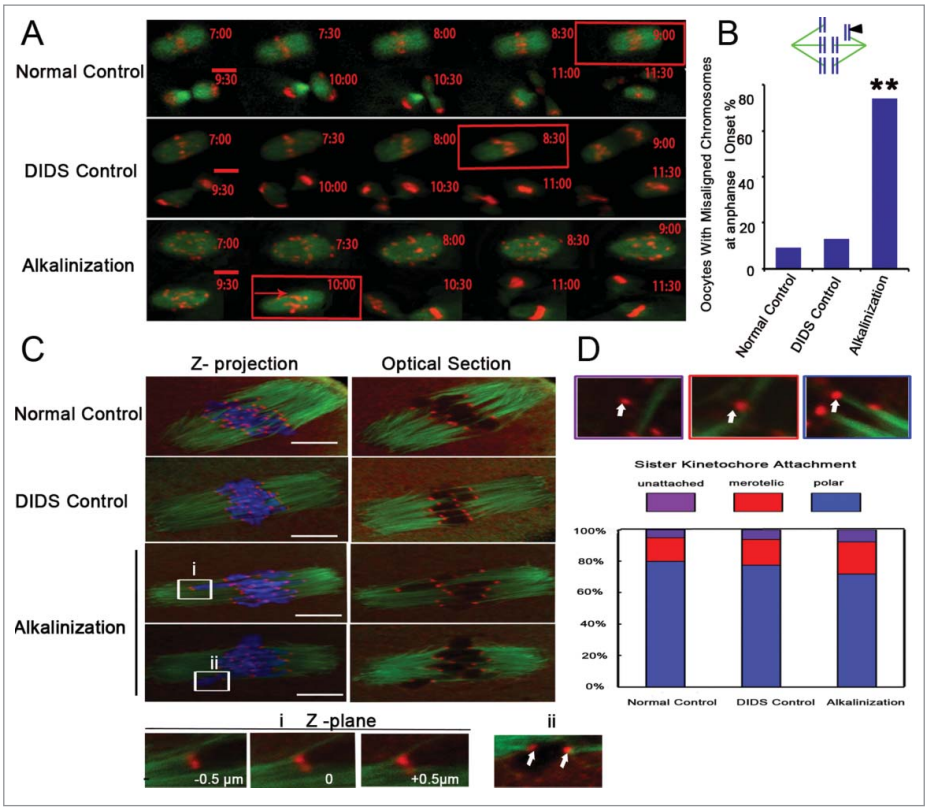

Figure 6. Chromosome misarrangement and normal KT-MT attachment in alkaline oocytes. (A) Chromosomes and spindles were labeled with H_2B-red and Map7-green, respectively. The images of chromosomes and spindles were captured at 30-min intervals over 16-17 h. The time of anaphase I onset was marked with a *red square*. Chromosom misarrangement was marked with a *red arrow*. Movies for the normal control and the alkalinization-treated groups are available (Supplemental Videos S1, S2). Scale bar, 10 μm. (B) Chromosome misalignment is shown in a model and marked with a *black triangle*. Oocytes with misaligned chromosomes were confirmed at the onset of anaphase I. The data were analyzed using a chi-square test. (C) Representative images of the 3 groups are shown. The iKT distance of misaligned sister pairs was more than 10 μm, and its one kinetochore had an amphitelic attachment (i). Misaligned sister pairs had a single polar attachment, marked with *a white arrow* (ii). DNA: blue, kinetochore: red, α-tubulin: green. Scale bar, 10 μm. (D) Analysis of attachment types in oocytes from the normal control, DIDS control and alkalinization-treated groups. A total of 800 univalent attachments from 20 normal-control oocytes, 840 univalent attachments from 21 DIDS-control oocytes, and 1000 univalent attachments from 25 alkaline-treated oocytes were classified from 3 experimental replicates. Each attachment type was shown using *white arrow*.

mice.[27,30] Therefore, in the present study, *AE2* mRNA expression level was analyzed in GV oocytes of 1- and 12-month-old mice. *AE2* mRNA expression level in GV oocytes was significantly decreased in aged mice (Fig. 3D). Pan and his colleagues suggested that ~5 % of the transcripts are differentially expressed in GV oocytes obtained from aged mice (60–70 weeks) compared to oocytes obtained from young females (6–12 weeks) using microarray expression profiling.[1] In human GV oocytes, aging can also lead to the degradation of the Bub1 and Mad2 messages.[35] Therefore, we speculate that the deficiency in *AE2* transcripts may explain the deterioration of HCO_3^-/Cl^- exchanger activity in aged GV oocytes.

Most cellular processes are acutely pH-sensitive, including embryo metabolism, mitochondrial function and cytoskeletal regulation.[20,36] For example, growth and proliferation are impaired in some pH_i regulation-compromised cells when the pH_i is disturbed.[37,38] Moreover, small changes (0.3-0.4 units) in the pH_i induce dramatic differences in actin filament assemblies and architectures.[39] Our results support an additional novel role of pH_i dysregulation that leads to the chromosome misarrangement and the increase in aneuploidy during oocyte maturation (Figs. 6A, B and 4D). It was previously determined that sister chromatids are linked to one another during DNA replication by cohesin complexes.[40,41] Any precocious loss of cohesion could cause aneuploidy in meiosis.[3,42] A reduced cohesin subunit causes the greater sister inter-kinetochore distances.[3] In the present study, we found that SMC3 protein level was dramatically reduced in MI oocytes with increased pH_i (Fig. 5A and B). Consistent with this result, the increase in pH_i caused increases in aneuploidy and sister iKT distances in young oocytes (Fig. 4C and D), which are associated with the reduction in cohesion.[3,32] Altered pH_i has been experimentally shown to change protein structure and, thus, to alter protein-protein binding affinity, change protein stability, modify protein function, and alter subcellular localization.[39] Although there are limited structural analyses of pH-dependent protein-DNA binding,[43] electrostatic interactions are very important in protein-DNA binding.[39] Therefore, we speculate that the increased pH_i in oocytes may give rise to the increases in aneuploidy and sister iKT distance via impairing the ring structure of the cohesin complex wrapped around the chromosome arms and centromeres. However, how the increased pH_i in oocytes affect the structure of the cohesin complex still require further study.

It is well known that aneuploidy of meiotic origin increases dramatically with maternal age.[3,32,41] Our results showed that the aneuploid rate of MII oocytes in 12-month-old mice was significantly higher than that in 1-month-old mice (Fig. 1A). Current evidence suggests that the deterioration of cohesion with increasing maternal age is a leading cause of age-related

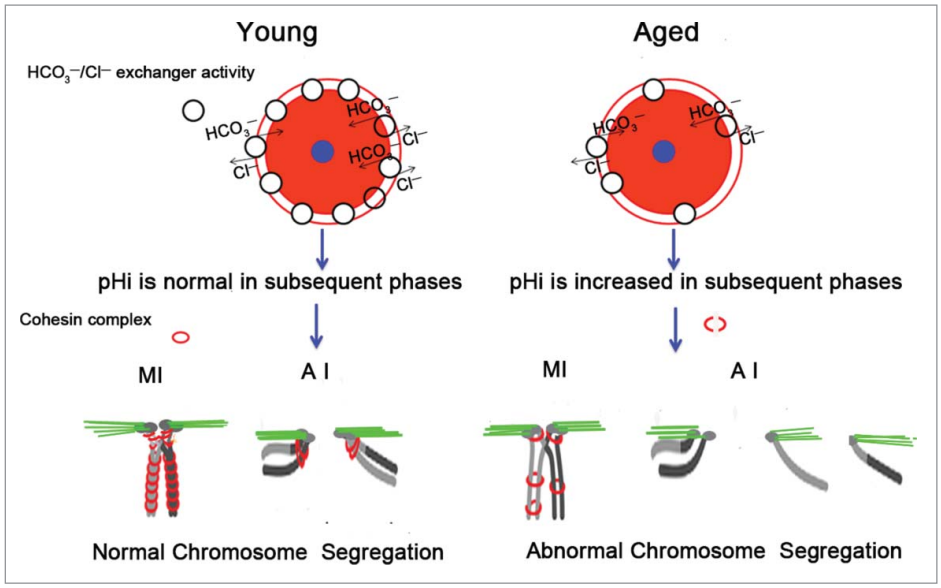

Figure 7. Schematic representation of the involvement of increased pH_i in aneuploidy in old oocytes. Aging causes decreased HCO_3^-/Cl^- exchanger activity in full-grown GV oocytes, which have the strongest HCO_3^-/Cl^- exchanger activity of the oocyte phases.[26,27] Therefore, in subsequent phases of aged oocytes, anions cannot be excluded in a timely manner to the extracellular compartment due to reduced activity of the HCO_3^-/Cl^- exchanger, leading to an increase in the oocyte pH_i. The increased pH_i of aged oocytes might affect the cohesin subunit-subunit binding affinity, change its stability, modify its function, and alter its subcellular localization, among other effects. Finally, the increased pH_i of aged oocytes gives rise to the deterioration of the cohesin wrapped around the chromosome, leading to increased aneuploidy. The small blue circle represents the nucleus, and the pink circle represents the cytoplasm.

aneuploidy,[3-5,41] but what factors cause the loss of cohesion in aged oocytes is still unknown. Jessberger suggests some assumptions, including cleavage or spontaneous hydrolysis of a single peptide within the large cohesin ring during the long period of arrest, low separase activity might contribute to the significant loss of cohesion in aged oocytes, and the change in cohesin subunit acetylation in aged oocytes.[5] In this study, we found that increased pH_i in young oocytes can cause aneuploidy associated with the deterioration of cohesion and that aged oocytes have a high pH_i and aneuploidy. Combined with the change of pH_i impacting protein structure,[39] it would seem reasonable that the dysregulation of pH_i in aged oocytes might damage protein-protein binding affinity or protein localization of the cohesin complex, leading to the deterioration of chromosome cohesion and increased chromosome aneuploidy.

In conclusion, mouse oocyte pH_i increases with advancing age, which may be a result of the decreases in HCO_3^-/Cl^- exchanger activity and *AE2* mRNA expression in aged oocytes. The elevated pH_i in young oocytes can cause the increase in aneuploidy associated with the loss of cohesion. We speculate that in aged oocytes, the increase in pH_i might damage the cohesin complex structure, resulting in chromosome misalignment and increased aneuploidy (Fig. 7). The identification of an association between loss of cohesion and increased pH_i would provide a new insight into age-related aneuploidy.

Materials and methods

All experimental protocols and animal handling procedures were conducted in accordance with the guidelines and procedures approved by the Institutional Animal Care and Use Committee (IACUC) of the Institute of Zoology (IOZ), University of Chinese Academy of Sciences (UCAS).

Chemicals and solutions

All chemicals and drugs were purchased from Sigma (St. Louis, MO, USA), unless otherwise indicated. BCECF-AM (2′,7′-bis-(2-carboxyethyl)-5-(and-6)-carboxyfluorescein, acetoxymethyl ester) solution, nigericin and valinomycin were obtained from Molecular Probes (Eugene, OR, USA). Rec8 polyclonal antibody was purchased from Proteintech (Chicago, IL, USA, 10793-1-AP). Human centromere (CREST) autoimmune serum was acquired from Immunovision (HCT-010, Arkansas, USA). Stock solutions were prepared in water and include the following: [dibutyryladenosine 3,5-cyclic monophosphate (dbcAMP)], ethanol (nigericin), dimethyl sulfoxide (DMSO; SNARF-1-AM, valinomycin, monastrol), and 0.1 M $KHCO_3$ (DIDS).

All media were based on the KSOM mouse embryo culture medium.[44] For all fluorophore-loading and pH_i measurements, 9 mM Na lactate was replaced with NaCl (total 104 mM NaCl and 1 mM Na lactate), and bovine serum albumin (BSA) was excluded. The medium is designated here as pH-KSOM. Cl^--free medium was produced by replacing all Cl^- salts with corresponding gluconate salts. The HCO_3^-/CO_2-buffered media were equilibrated with 5 % CO_2/air.

Oocyte collection, culture and alkalinization treatment

All studies were performed using Swiss CD1 outbred females (Vital River Laboratory Animal Technology Co. Ltd.). The mice were sacrificed by cervical dislocation 48 h after intraperitoneal injection of 5 IU of equine chorionic gonadotropin (eCG, Ningbo Hormone Product Co. Ningbo, Zhejiang Province, China). Full-grown GV oocytes were released by puncturing ovaries with a 28-gauge microinjection needle and then collected by mouth pipette in M2 medium supplemented with

100 mM dbcAMP. Cumulus cells were subsequently removed by repeated pipetting through a narrow-bore pipette. Full-grown GV oocytes were matured in an M16 medium for 2-2.5, 7.5-8 and 16-17 h to collect GVBD, MI and MII phases, respectively; the maturation process took place in an incubator at 37°C with 5 % CO_2 in air. According to the rate of the first polar body extrusion (PBE) (Supplemental Fig. S1B), we determined that 60 μM DIDS, an inhibitor of HCO_3^-/Cl^- exchangers (Supplemental Fig. S1A), would be added to the maturation medium. To make the oocytes alkalosis, the pH_i values of their GV stages were elevated through treatment in Cl^--free medium for 10 min. The oocytes were then cultured in an M16 medium with an additional 60 μM DIDS, as shown in Fig. 3A.

pH_i measurements

pH_i measurements were performed using a quantitative imaging microscopy system (Velocity software 6.0.1, Perkin Elmer), as previously described.[27,45] Briefly, pH_i was measured using BCECF, which was loaded as the acetoxymethyl ester derivative (BCECF-AM, ~5 μM, 30 min). BCECF was illuminated using light with wavelengths of 488 nm and 440 nm, and emission was monitored at 535 nm. The ratio of the 2 intensities (488/440) was calculated by dividing the images after background subtraction. Where shown, the exemplar image is of the 488-nm emission (Fig. 2A). Calibration was performed using the nigericin/high K^+ method with valinomycin added to collapse the K^+ gradient.[24,46] The pH_i was determined in KSOM after a 15-min stabilization period. The pH_i values were averaged for oocytes within 5-μm increments for each experiment. dbcAMP (100 μM) was included in some experiments to prevent spontaneous oocyte maturation. All measurements were performed in a temperature- and atmosphere-controlled chamber (37°C, 5 % CO_2/air).

Cl^- removal assay for HCO_3^-/Cl^- exchanger activity

HCO_3^-/Cl^- exchange activity was quantified using the Cl^- removal method. Upon exposure to the Cl^--free solution, the HCO_3^-/Cl^- exchanger runs in reverse, causing intracellular alkalinization due to HCO_3^- influx. Thus, a pH_i increase upon Cl^- removal indicates HCO_3^-/Cl^- exchanger activity, and the initial rate of alkalinization provides a quantitative measure of activity.[47] Here, BCECF-containing oocytes were placed in the chamber and equilibrated for 15 min, and measurements were then taken for 10 min, after which the solution was changed to Cl^--free, low-lactate KSOM. The initial rate of intracellular alkalinization upon Cl^- removal was determined using linear regression (Sigma Plot 8.0, Chicago, IL, USA), and exchanger activity was reported as the change in pH_i per min (pHU/min). This assay for HCO_3^-/Cl^- exchanger activity has been extensively described and validated in mouse oocytes.[27,30]

Immunofluorescence, imaging, measurement of iKT distance and chromosome counting

Experiments were conducted as previously reported.[3,33,48,49] Oocytes were fixed in a solution of 4 % paraformaldehyde and 0.25 % Triton-X in PBS for 40 min. Blocking was performed in PBS with 3 % BSA for 60 min at 37°C. Antibodies were used for immunolabelling and included human anti-centromere (1:200) and mouse anti-α-tubulin (1:200). Alexa-labeled secondary antibodies were used as appropriate. For the analysis of cold-stable microtubules, oocytes were exposed to ice-cold M2 medium for 10 min immediately prior to fixation. For in situ chromosome counts, MII oocytes were treated for 1.5 h in M16 medium supplemented with 100 mM monastrol before fixation. Oocytes were then stained with DAPI for 10 min, and images were collected with a spinning disk confocal at 0.4-μm intervals to span the entire region of the spindle using a 63 × 1.4 NA oil immersion objective (LSM 780). Inter-kinetochore distances were measured from the inner edges of all sister kinetochore pairs (Fig. 4B) and were determined based on a CREST signal using Image J software (NIH). To obtain chromosome and kinetochore counts and the attached orientation of the kinetochore and microtubule of each egg, serial confocal sections were analyzed using the ZEN 2011 Viewer (Zeiss) and NIH.

For chromosome spreads, oocytes were mounted on glass slides and fixed in a solution of 1 % paraformaldehyde in distilled H_2O (pH 9.2) containing 0.15 % Triton X-100 and 3 mM dithiothreitol after the zona pellucida were removed by a brief exposure to acid Tyrode's solution. The slides were left to dry and then blocked with 1 % BSA in PBS for 1 h at room temperature. The slides were incubated with SMC3 and centromere antibody overnight at 4°C. After brief washes with PBS, the slides were then incubated with secondary antibody for 2 h at room temperature. Following DNA staining with DAPI, the slides were mounted on cover glass and examined via immunofluorescence microscopy (Zeiss LSM 780). Fluorescence intensities were calculated using blue ZEN 2012 software. The values are presented as the means ± SEM.

cDNA preparation and real-time polymerase chain reaction analysis

Total RNA was isolated from 80 GV oocytes and treated with DNase I to eliminate DNA contamination. The RNA was then reverse transcribed using the M-MLV Reverse Transcriptase kit (Promega) following the manufacturer's instructions. Real-time polymerase chain reaction analysis was performed as described previously[50] to quantify the steady-state mRNA levels of *AE2* and the housekeeping gene *GADPH* (endogenous control). Calculations of the relative fold changes in *AE2* were performed using the $2^{-\Delta\Delta Ct}$ method, as described previously.[50] The values are presented as the means ± SEM. The *GADPH* forward primer was TTGTCTCCTGCGACTTCAACA, and the reverse primer was ACCA GGAAATGAGCTTGACAAAG. The *AE2* forward primer was CCCAGCCTG GACATCGAAG, and the reverse primer was CAGGAACATCCTC AAATCG GTG.

Preparation of cRNA, microinjection and live cell imaging

The plasmids pRN3-H_2B-RFP1 and pRN3-MAP7-eGFP were gifts from Greg Fitzharris. The plasmids were linearized via digestion with Sfi I. Then, 5′-capped cRNAs were synthesized using T3 mMessage mMachine (AM1348) according to the manufacturer's instructions. cRNA (1500 ng/μl) was dissolved in nuclease-free water and stored at −80°C. cRNA was then

injected at pipette concentrations of 300 ng/μl for MAP7-GFP and 200 ng/μl for H_2B-RFP. Approximately 1.5 pg MAP7-GFP and 0.3 pg H_2B-RFP were injected into GV oocytes.

The full-grown and naked GV oocytes were cultured for 2-3 h for cRNA expression in M16 medium supplemented with 100 μM dbcAMP after microinjection. These GV oocytes were divided into 3 groups for live cell imaging. One group was treated in Cl^--free media for 10 min and was then removed to culture medium containing an additional 60 μM DIDS, one group was cultured directly in medium supplemented with 60 μM DIDS, and another group was cultured in normal culture medium without any addition and treatment. For time-lapse imaging, oocytes were housed in an air-controlled environment at 37°C and 5 % CO_2. Images were captured every 30 mins with a z-resolution of 2.0 μm. Tracking lasted for 16-17 h using the PerkinElmer UltraView-Vox 20 × (NA 1.4) objective on a spinning disk confocal microscope. Images were analyzed using Image J.

Statistical analysis

All experiments were repeated at least 3 times. Dichotomous data were analyzed using a chi-square test. Other data in the present study were analyzed using Student's t-test in SPSS (Statistical Package for the Social Sciences) 19.0 software (SPSS, Inc., Chicago, IL, USA). $P < 0.05$ and $P < 0.01$ values were considered statistically significant.

Abbreviations

AE	anion exchanger
DIDS	4,4′-diisothiocyanatostilbene-2,2′-disulfonate
GV	germinal vesicle
GVBD	germinal vesicle breakdown
iKT	inter-kinetochore
KT-MT	kinetochore-microtubule
MI	metaphase I
MII	metaphase II
PB1	first polar body
PBE	first polar body extrusion
pH_i	intracellular pH
SMC3	structural maintenance of chromosomes 3

Disclosure of potential conflicts of interest

No potential conflicts of interest were disclosed.

Acknowledgments

We thank Jay M. Baltz for technical support in the measurement of pH_i and for offering the recipe for the KSOM-related solution, Greg Fitzharris for providing plasmids pRN3-H2B-RFP1 and pRN3-MAP7-eGFP and Heng-Yu Fan for the SMC3 antibody. We thank Chawnshang Chang (University of Rochester Medical Center, Rochester, NY 14642. E-Mail: chang@urmc.rochester.edu) for reviewing this manuscript. We thank NPG language editing for proofreading the manuscript.

Funding

This work was supported by the Major Research Plan "973" Project (2012CB944702) and Grants from the National Natural Science Foundation of China (31501953, 31501198, 31501161, 31471352, 31471400, 81270662) and Academician Workstation support (Shenyang, Changsha and Shan Dong).

References

[1] Pan H, Ma P, Zhu W, Schultz RM. Age-associated increase in aneuploidy and changes in gene expression in mouse eggs. Dev Biol 2008; 316:397-407; PMID:18342300; http://dx.doi.org/10.1016/j.ydbio.2008.01.048

[2] Nagaoka SI, Hassold TJ, Hunt PA. Human aneuploidy: mechanisms and new insights into an age-old problem. Nat Rev Genet 2012; 13:493-504; PMID:22705668; http://dx.doi.org/10.1038/nrg3245

[3] Chiang T, Duncan FE, Schindler K, Schultz RM, Lampson MA. Evidence that weakened centromere cohesion is a leading cause of age-related aneuploidy in oocytes. Curr Biol 2010; 20:1522-8; PMID:20817534; http://dx.doi.org/10.1016/j.cub.2010.06.069

[4] Chiang T, Schultz RM, Lampson MA. Meiotic origins of maternal age-related aneuploidy. Biol Reprod 2012; 86:1-7; PMID:21957193; http://dx.doi.org/10.1095/biolreprod.111.094367

[5] Jessberger R. Age-related aneuploidy through cohesion exhaustion. EMBO Rep 2012; 13:539-46; PMID:22565322

[6] Jones KT, Lane SI. Molecular causes of aneuploidy in mammalian eggs. Development 2013; 140:3719-30; PMID:23981655; http://dx.doi.org/10.1242/dev.090589

[7] Fu X, Cheng J, Hou Y, Zhu S. The association between the oocyte pool and aneuploidy: a comparative study of the reproductive potential of young and aged mice. J Assist Reprod Genet 2014; 31:323-31; PMID:24362910; http://dx.doi.org/10.1007/s10815-013-0160-5

[8] Sakakibara Y, Hashimoto S, Nakaoka Y, Kouznetsova A, Hoog C, Kitajima TS. Bivalent sep -aration into univalents precedes age-related meiosis I errors in oocytes. Nat Commun 2015; 6:7550; PMID:26130582

[9] Brieno-Enriquez MA, Cohen PE. Double trouble in human aneuploidy. Nat Genet 2015; 47:696-8; PMID:26111508; http://dx.doi.org/10.1038/ng.3344

[10] Brar GA, Amon A. Emerging roles for centromeres in meiosis I chromosome segregation. Nat Rev Genet 2008; 9:899-910; PMID:18981989; http://dx.doi.org/10.1038/nrg2454

[11] Hauf S, Watanabe Y. Kinetochore orientation in mitosis and meiosis. Cell 2004; 119:317-27; PMID:15507205; http://dx.doi.org/10.1016/j.cell.2004.10.014

[12] Garcia-Cruz R, Brieno MA, Roig I, Grossmann M, Velilla E, Pujol A, Cabero L, Pessarrodona A, Barbero JL, Garcia Caldes M. Dynamics of cohesin proteins REC8, STAG3, SMC1 beta and SMC3 are consistent with a role in sister chromatid cohesion during meiosis in human oocytes. Hum Reprod 2010; 25:2316-27; PMID:20634189; http://dx.doi.org/10.1093/humrep/deq180

[13] Wood AJ, Severson AF, Meyer BJ. Condensin and cohesin complexity: the expanding repertoire of functions. Nat Rev Genet 2010; 11:391-404; PMID:20442714; http://dx.doi.org/10.1038/nrg2794

[14] Takahashi T, Saito H, Hiroi M, Doi K, Takahashi E. Effects of aging on inositol 1,4,5-triphosphate-induced Ca^{2+} release in unfertilized mouse oocytes. Mol Reprod Dev 2000; 55:299-306; PMID:10657049; http://dx.doi.org/10.1002/(SICI)1098-2795(200003)55:3%3c299::AID-MRD8%3e3.0.CO;2-G

[15] Takahashi T, Takahashi E, Igarashi H, Tezuka N, Kurachi H. Impact of oxidative stress in aged mouse oocytes on calcium oscillations at fertilization. Mol Reprod Dev 2003; 66:143-52; PMID:12950101; http://dx.doi.org/10.1002/mrd.10341

[16] Miao YL, Kikuchi K, Sun QY, Schatten H. Oocyte aging: cellular and molecular changes, developmental potential and reversal possibility. Hum Reprod Update 2009; 15:573-85; PMID:19429634; http://dx.doi.org/10.1093/humupd/dmp014

[17] Simsek-Duran F, Li F, Ford W, Swanson RJ, Jones HW Jr, Castora FJ. Age-associated metabolic and morphologic changes in mitochondria of individual mouse and hamster oocytes. PLoS One 2013; 8:e64955; PMID:23741435; http://dx.doi.org/10.1371/journal.pone.0064955

[18] Alper SL. The band 3-related AE anion exchanger gene family. Annu Rev Physiol 1991; 53:549-64; PMID:2042971; http://dx.doi.org/10.1146/annurev.ph.53.030191.003001

[19] Orlowski J, Grinstein S. Na^+/H^+ exchangers of mammalian cells. J Biol Chem 1997; 272:22373-6; PMID:9278382; http://dx.doi.org/10.1074/jbc.272.36.22373
[20] Roos A, Boron WF. Intracellular pH. Physiol Rev 1981; 61:296-434; PMID:7012859
[21] Alper SL. Molecular physiology of SLC4 anion exchangers. Exp Physiol 2006 ;91:153-61; PMID:16239253; http://dx.doi.org/10.1113/expphysiol.2005.031765
[22] Romero MF, Fulton CM, Boron WF. The SLC4 family of HCO_3^- transporters. Pflugers Arch 2004; 447:495-509; PMID:14722772; http://dx.doi.org/10.1007/s00424-003-1180-2
[23] Romero MF, Chen AP, Parker MD, Boron WF. The SLC4 family of bicarbonate (HCO_3^-/Cl^-) transporters. Mol Aspects Med 2013; 34:159-82; PMID:23506864; http://dx.doi.org/10.1016/j.mam.2012.10.008
[24] Phillips KP, Baltz JM. Intracellular pH regulation by HCO_3^-/Cl^- exchange is activated during early mouse zygote development. Dev Biol 1999; 208:392-405; PMID:10191053; http://dx.doi.org/10.1006/dbio.1999.9199
[25] Zhao Y, Chauvet PJ, Alper SL, Baltz JM. Expression and function of bicarbonate/chloride exchangers in the preimplantation mouse embryo. J Biol Chem 1995; 270:24428-34; PMID:7592657; http://dx.doi.org/10.1074/jbc.270.41.24428
[26] Erdogan S, FitzHarris G, Tartia AP, Baltz JM. Mechanisms regulating intracellular pH are activated during growth of the mouse oocyte coincident with acquisition of meiotic competence. Dev Biol 2005; 286:352-60; PMID:16150436; http://dx.doi.org/10.1016/j.ydbio.2005.08.009
[27] Fitzharris G, Baltz JM. Granulosa cells regulate intracellular pH of the murine growing oocyte via gap junctions: development of independent homeostasis during oocyte growth. Development 2006; 133:591-9; PMID:16407396; http://dx.doi.org/10.1242/dev.02246
[28] FitzHarris G, Siyanov V, Baltz JM. Granulosa cells regulate oocyte intracellular pH against acidosis in preantral follicles by multiple mechanisms. Development 2007; 134:4283-95; PMID:17978006; http://dx.doi.org/10.1242/dev.005272
[29] Phillips KP, Petrunewich MA, Collins JL, Baltz JM. The intracellular pH-regulatory HCO_3^-/Cl^- exchanger in the mouse oocyte is inactivated during first meiotic metaphase and reactivated after egg activation via the MAP kinase pathway. Mol Biol Cell 2002; 13:3800-10; PMID:12429825; http://dx.doi.org/10.1091/mbc.E02-04-0242
[30] Zhou C, Tiberi M, Liang B, Alper SL, Baltz JM. HCO_3^-/Cl^- exchange inactivation and reactivation during mouse oocyte meiosis correlates with MEK/MAPK -regulated Ae2 plasma membrane localization. PLoS One 2009; 4:e7417; PMID:19823673; http://dx.doi.org/10.1371/journal.pone.0007417
[31] FitzHarris G, Baltz JM. Regulation of intracellular pH during oocyte growth and maturation in mammals. Reproduction 2009; 138:619-27; PMID:19520797; http://dx.doi.org/10.1530/REP-09-0112
[32] Merriman JA, Jennings PC, McLaughlin EA, Jones KT. Effect of aging on superovulation efficiency, aneuploidy rates, and sister chromatid cohesion in mice aged up to 15 months. Biol Reprod 2012; 86:49; PMID:22053097; http://dx.doi.org/10.1095/biolreprod.111.095711
[33] Shomper M, Lappa C, FitzHarris G. Kinetochore microtubule establishment is defective in oocytes from aged mice. Cell Cycle 2014; 13:1171-9; PMID:24553117; http://dx.doi.org/10.4161/cc.28046
[34] Damaghi M, Wojtkowiak JW, Gillies RJ. pH sensing and regulation in cancer. Front Physiol 2013; 4:370; PMID:24381558; http://dx.doi.org/10.3389/fphys.2013.00370
[35] Steuerwald N, Cohen J, Herrera RJ, Sandalinas M, Brenner CA. Association between spindle assembly chechpoint expression and maternal age in human oocytes. Mol Hum Reprod 2001; 7:49-55; PMID:11134360; http://dx.doi.org/10.1093/molehr/7.1.49
[36] Bavister B. Culture of preimpantation embryos: facts and artifacts. Hum Reprod Update 1995; 1:91-148; PMID:15726768; http://dx.doi.org/10.1093/humupd/1.2.91
[37] Grinstein S, Rotin D, Mason MJ. Na^+/H^+ exchange and growth factor-induced cytosolic pH changes. Role in cellular proliferation. Biochim Biophys Acta 1989; 988:73-97; PMID:2535787; http://dx.doi.org/10.1016/0304-4157(89)90004-X
[38] Kapus A, Grinstein S, Wasan S, Kandasamy R, Orlowski J. Functional characterization of three isoforms of the Na^+/H^+ exchanger stably expressed in Chinese hamster ovary cells. ATP dependence, osmotic sensitivity, and role in cell proliferation. J Biol Chem 1994; 269:23544-52; PMID:8089122
[39] Schonichen A, Webb BA, Jacobson MP, Barber DL. Considering protonation as a posttranslational modification regulating protein structure and function. Annu Rev Biophys 2013; 42:289-314; PMID:23451893; http://dx.doi.org/10.1146/annurev-biophys-050511-102349
[40] Tachibana-Konwalski K, Godwin J, van der Weyden L, Champion L, Kudo NR, Adams DJ, Nasmyth K. Rec8-containing cohesin maintains bivalents without turnover during the growing phase of mouse oocytes. Genes Dev 2010; 24:2505-16; PMID:20971813; http://dx.doi.org/10.1101/gad.605910
[41] Lister LM, Kouznetsova A, Hyslop LA, Kalleas D, Pace SL, Barel JC, Nathan A, Floros V, Adelfalk C, Watanabe Y, et al. Age-related meiotic segregation errors in mammalian oocytes are preceded by depletion of cohesin and Sgo2. Curr Biol 2010; 20:1511-21; PMID:20817533; http://dx.doi.org/10.1016/j.cub.2010.08.023
[42] Hodges CA, Revenkova E, Jessberger R, Hassold TJ, Hunt PA. SMC1beta-deficient female mice provide evidence that cohesins are a missing link in age-related nondisjunction. Nat Genet 2005; 37:1351-55; PMID:16258540; http://dx.doi.org/10.1038/ng1672
[43] Lundback T, van Den Berg S, Hard T. Sequence-specific DNA binding by the glucocorticoid receptor DNA-binding domain is linked to a salt-dependent histidine protonation. Biochemistry 2000; 39:8909-16; PMID:10913303; http://dx.doi.org/10.1021/bi000231i
[44] Lawitts JA, Biggers JD. Culture of preimplantation embryos. Methods Enzymol 1993; 225:153-64; PMID:8231853; http://dx.doi.org/10.1016/0076-6879(93)25012-Q
[45] Dale B, Menezo Y, Cohen J, DiMatteo L, Wilding M. Intracellular PH regulation in the human oocyte. Hum Reprod 1998; 13:964-70; PMID:9619555; http://dx.doi.org/10.1093/humrep/13.4.964
[46] Baltz JM, Biggers JD, Lechene C. Apparent absence of Na+/H+ antiport activity in the two- cell mouse embryo. Dev Biol 1990; 138:421-9; PMID:2156738; http://dx.doi.org/10.1016/0012-1606(90)90208-Z
[47] Nord EP, Brown SE, Crandall ED. Cl^-/HCO_3^- exchange modulates intracellular pH in rat type II alveolar epithelial cells. J Biol Chem 1988; 263:5599-606; PMID:3356700
[48] Cheng JM, Jia BY, Wu TY, Zhou GB, Hou YP, Fu XW, Zhu SE. Effects of vitrification for germinal vesicle and metaphase II oocytes on subsequent centromere cohesion and chromosome aneuploidy in mice. Theriogenology 2014; 82:495-500; PMID:24930605; http://dx.doi.org/10.1016/j.theriogenology.2014.05.009
[49] Hodges CA, Hunt PA. Simultaneous analysis of chromosomes and chromosome-associated proteins in mammalian oocytes and embryos. Chromosoma 2002; 111:165-9; PMID:12355205; http://dx.doi.org/10.1007/s00412-002-0195-3
[50] Su YQ, Sugiura K, Woo Y, Wigglesworth K, Kamdar S, Affourtit J, Eppig JJ. Selective degradation of transcripts during meiotic maturation of mouse oocytes. Dev Biol 2007; 302:104-17; PMID:17022963; http://dx.doi.org/10.1016/j.ydbio.2006.09.008